

Manuscript Details

Manuscript number	JPHOTOCHEM_2016_803
Title	Characterization of dye-sensitized solar cells using five pure anthocyanidin 3-O-glucosides possessing different chromophores
Article type	Full length article

Abstract

Five anthocyanins, pelargonidin, cyanidin, delphinidin, petunidin and malvidin 3-O-glucosides, possessing different substitution patterns in the B-ring of the anthocyanidin chromophore were isolated from various plant materials. Using the pure pigments, dye-sensitized solar cells (DSSCs) were fabricated, and then their cell-color and conversion efficiencies ($\eta\%$) were compared. After optimization of the fabrication conditions, all the cells showed 0.6-1.4% conversion efficiency under AM 1.5. Among them, petunidin 3-O-glucoside gave the highest efficiency of 1.42% following the addition of deoxycholic acid (DCA) as an additive; however, removal of the glucosyl unit decreased the efficiency. The cell colors of cyanidin, delphinidin, and petunidin 3-O-glucoside showed bluer with relatively high $\eta\%$ ($>1\%$) values compared with those of pelargonidin and malvidin 3-O-glucoside. Those phenomena may indicate that the former three pigments may attach to TiO₂ through the catechol moiety of the B-ring of the chromophores. Time-dependent density functional theory (TD-DFT) calculations were performed on model systems comprising anthocyanidin dyes on a (TiO₂)₃₈ cluster to characterize the photo-absorption properties of DSSCs.

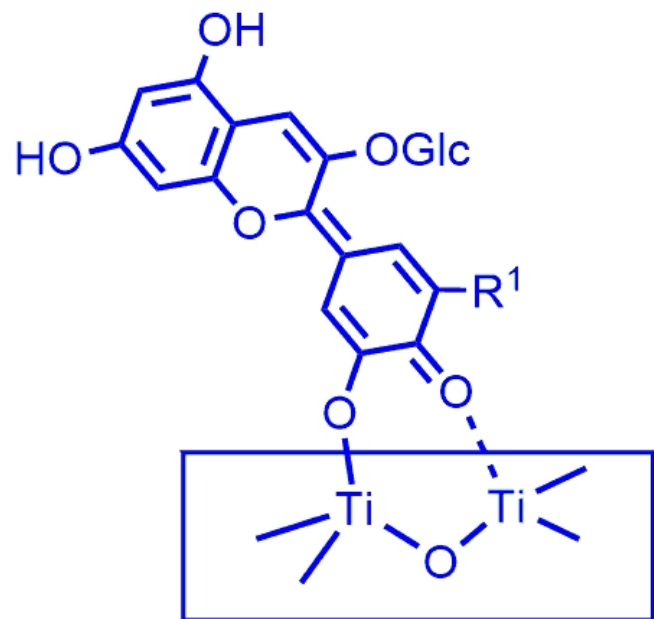
Keywords	anthocyanin; dye-sensitized solar cell; natural pigment; petunidin 3-O-glucoside; TD-DFT calculation; (TiO ₂) ₃₈ cluster
Manuscript region of origin	Asia Pacific
Corresponding Author	Kumi Yoshida
Order of Authors	Yuki Kimura, Takeshi Maeda, Satoru Iuchi, Nobuaki Koga, Yasujiro Murata, Atsushi Wakamiya, Kumi Yoshida
Suggested reviewers	Naohiko Kato, Shuji Hayase, Fernando Pina

Submission Files Included in this PDF

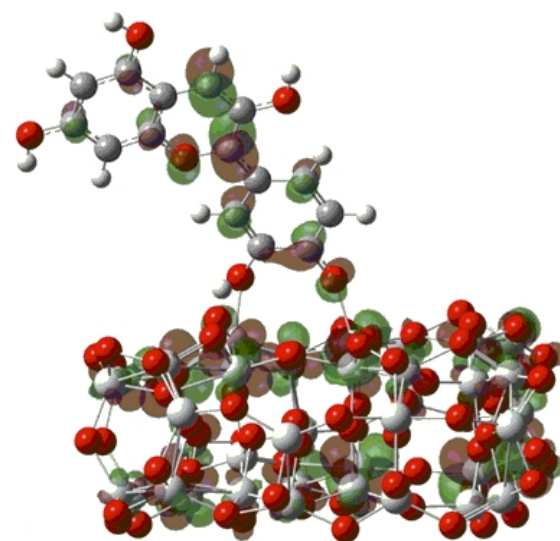
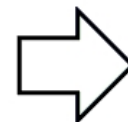
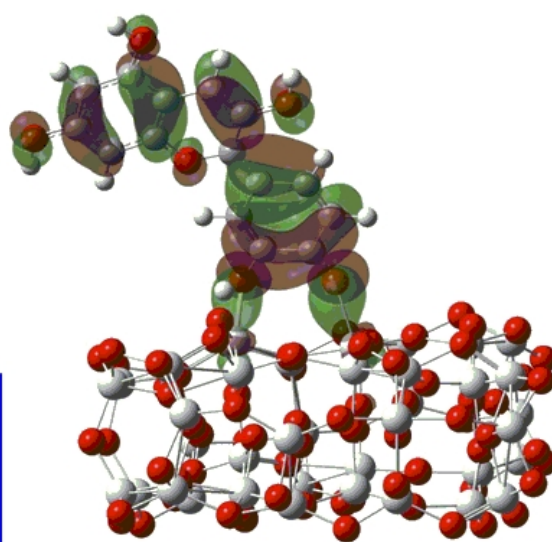
File Name [File Type]

Cover_Letter-Yoshida.docx [Cover Letter]
Response_Letter-Yoshida.docx [Response to reviewers]
Graphical_abstract-Yoshida.tif [Graphical Abstract]
Revised-JPHOTOCHEM_2016_803.doc [Manuscript]
Fig. 1.jpg [Figure]
Fig. 2.jpg [Figure]
Fig3-Yoshida.jpg [Figure]
Fig4-Yoshida.jpg [Figure]
Supplementary_Material-Yoshida.pdf [Figure]
Highlights-Yoshida.docx [Highlights]

To view all the submission files, including those not included in the PDF, click on the manuscript title on your EVISE Homepage, then click 'Download zip file'.



R¹ = H, OH, OCH₃



cyanidin/(TiO₂)₃₈

Characterization of dye-sensitized solar cells using five pure anthocyanidin 3-*O*-glucosides possessing different chromophores

Yuki Kimura ^a, Takeshi Maeda ^a, Satoru Iuchi ^a, Nobuaki Koga ^a, Yasujiro Murata ^b, Atsushi Wakamiya ^b, Kumi Yoshida ^{a,*}

^a Graduate School of Information Science, Nagoya University, Chikusa, Nagoya 464-8601, Japan

^b Institute for Chemical Research, Kyoto University, Uji, Kyoto 611-0011, Japan

*Corresponding author: FAX +81-52-789-5638; E-mail yoshidak@is.nagoya-u.ac.jp

Abstract

Five anthocyanins, namely, pelargonidin, cyanidin, delphinidin, petunidin and malvidin 3-*O*-glucosides, possessing different substitution patterns in the B-ring of the anthocyanidin chromophore were isolated from various plant materials. Dye-sensitized solar cells (DSSCs) were fabricated using the pure pigments, and then their cell colors and conversion efficiencies ($\eta\%$) were compared. After optimization of the fabrication conditions, all the cells showed 0.6-1.4% conversion efficiency under AM 1.5. Among them, petunidin 3-*O*-glucoside provided the highest efficiency of 1.42% following the addition of deoxycholic acid (DCA) as an additive; however, removal of the glucosyl unit decreased the efficiency. The cell colors of cyanidin, delphinidin, and petunidin 3-*O*-glucosides appeared bluer with relatively high $\eta\%$ (>1%) values compared with those of pelargonidin and malvidin 3-*O*-glucosides. These phenomena may indicate that the former three pigments may attach to TiO₂ through the catechol moiety of the B-ring of the chromophores. Time-dependent density functional theory (TD-DFT) calculations were performed on model systems consisting of anthocyanidin dyes on a (TiO₂)₃₈ cluster to characterize the photo-

absorption properties of DSSCs.

Keywords

Anthocyanin; Dye-sensitized solar cell; Natural pigment; Petunidin 3-*O*-glucoside; TD-DFT calculation; (TiO₂)₃₈ cluster

1. Introduction

Following the breakthrough of dye-sensitized solar cells (DSSCs) by Grätzel using an organic dye of a ruthenium-complex on TiO₂ particles [1,2], DSSCs are expected to be potent candidates among potential next-generation photovoltaic cells. However, the conversion efficiency ($\eta\%$) of DSSCs was demonstrated to be approximately 15% in the laboratory [3] and approximately 12% in practical usage [4,5], still lower than those of inorganic semiconductor solar cells: 27% with multi-junction cells [6] and 20% with perovskite cells [7,8]. However, DSSCs have several advantages compared with silicon-based and perovskite solar cells because DSSCs are cheaper; lighter; flexible; not black but rather colorful, from red, orange and blue with transparency; and free from toxic metals, such as the Pb contained in perovskite [9,10]. When rare-metal-free DSSCs are placed into practical use, they could be environmentally compatible solar cells. For this purpose, natural pigments, such as flavonoids, anthocyanins, and betalains, are promising due to their easy isolation from plants sources [9-20]. In addition, they can show beautiful colors.

Anthocyanins are flavonoid pigments found in flowers, fruits, leaves and roots [21-25]. One of the most interesting chemical characteristics of anthocyanins is that these pigments are under equilibrium in aqueous solutions and exhibit pH-dependent color changes; in strong acidic solutions, anthocyanin appears red; in neutral solutions, it appears purple; and in alkaline solutions, it appears blue. This result indicates that the structure of anthocyanin changes depending on the pH,

manifested as the red flavylium, the purple quinonoidal base and the blue quinonoidal base anion forms [21,23-26]. In addition, even under neutral conditions, anthocyanin presents a blue color upon complexation by metal ions such as Mg^{2+} , Fe^{3+} and Al^{3+} [21,23-25,27-29]. **These properties of anthocyanins are presumed to be suitable for DSSCs**; therefore, following the first study on the flower pigment of Anthurium [11], many investigations have been reported [10,12-18,20]. However, in previous studies, the $\eta\%$ value was less than 1.0%. Recently, an $\eta\%$ value of 2.9% was observed using red cabbage pigment [16], and a value of 2.2% was observed using synthetic anthocyanidin [30]. The source of anthocyanins is still dependent on naturally occurring plants, and most studies were conducted using mixtures of several anthocyanins with varying structures. This may hinder further investigations of DSSCs in terms of basic chemical and systematic studies.

We have been investigating the structure and color development of anthocyanins, and we have already clarified that colored beans are proper sources of simple anthocyanins; a large amount of anthocyanidin 3-*O*-glucosides possessing various chromophores are contained in kidney beans (*Phaseolus vulgaris* cv. Taishokintoki), such as pelargonidin 3-*O*-glucoside (**1**); in black soybeans (*Glycine max* cv. Hikariguro), such as cyanidin 3-*O*-glucoside (**2**); and in black turtle beans (*Phaseolus vulgaris*), such as delphinidin 3-*O*-glucoside (**3**), petunidin 3-*O*-glucoside (**4**) and malvidin 3-*O*-glucoside (**5**). Moreover, we have already established the purification procedure [31]. In this study, we prepared DSSCs using the aforementioned pure anthocyanins (**1-5**) to compare the color and $\eta\%$ of the cells depending on the chromophore structure and the numbers of hydroxy and methoxy substitutions. In addition, to obtain a better understanding of the properties of the present DSSC systems, density functional theory (DFT) calculations were performed on model systems consisting of anthocyanidin dyes on a $(TiO_2)_{38}$ cluster (dye/ $(TiO_2)_{38}$). For dyes, the aglycones of the five anthocyanins (**1-5**) were considered to be a suitable simplification, as was employed in previous reports [32,33]. The $(TiO_2)_{38}$ cluster model has

frequently been used to calculate the properties of DSSC systems [34].

2. Materials and methods

2.1. General

Ultraviolet-visible (UV-vis) absorption spectra were recorded on a JASCO V-560 spectrophotometer (cell length: 10 mm). The diffuse reflectance UV-vis spectra of the solid samples were obtained using an integrating sphere. For coating TiO₂ pastes (Solaronix Ti-Nanoxide) on FTO glass plates (Astellatech Co., Ltd., 75 mm × 25 mm × 1.8 mm thick), screen-printing equipment (WHT3, Mino International, Ltd. and HP-320, Newlong Seimitsu Kogyo Co., Ltd.) was used. Calcination of the TiO₂-coated FTO glass was performed using a furnace (FT-101W, Full-Tech Co., Ltd.). **N719 (Aldrich, 95%) was used as the standard dye.**

2.2 Purification and preparation of anthocyanins

Five anthocyanins, namely, pelargonidin 3-*O*-glucoside (**1**, Pg3G), cyanidin 3-*O*-glucoside (**2**, Cy3G), delphinidin 3-*O*-glucoside (**3**, Dp3G), petunidin 3-*O*-glucoside (**4**, Pt3G) and malvidin 3-*O*-glucoside (**5**, Mv3G), were extracted using an acidic methanol solution from the colored seed coats of kidney beans (*Phaseolus vulgaris* cv. Kintoki), black soybeans, (*Glycine max* cv. Hikariguro) and black turtle beans (*Phaseolus vulgaris*) and purified using XAD-7 column chromatography followed by preparative ODS-HPLC according to our previously reported procedure [31].

Two anthocyanidins, cyanidin (**6**, Cy) and petunidin (**7**, Pt), were prepared by acidic hydrolysis from **2** and **4**, respectively. Approximately 10 mg of **2** and **4** were dissolved in 10 mL of 6 M HCl aq. and heated at 60 °C for 20 h. After the reaction was completed, the obtained anthocyanidins were precipitated into a flask. Filtration followed by washing with water and drying

in vacuo provided dark red solids of **6** (11 mg, 48%) and **7** (9.4 mg, 79%) as HCl salts.

2.3 Determination of the molar absorptivity

The molar absorptivities (ϵ) of all the anthocyanins and anthocyanidins were calculated by measuring UV-vis spectra in 0.1% HCl-MeOH according to the equation $A = \epsilon \times c \times l$, where A is the absorbance at λ_{\max} , c is the concentration of dye (mol/L), and l is the path length (cm).

2.4 Preparation of DSSCs

We prepared the DSSCs in accordance with the method reported by Liu et al. with slight modifications [35]. TiO₂ films as photoanodes were prepared by screen-printing TiO₂ pastes with different particle diameters (11-400 nm) onto F-doped SnO₂ glass. After treating the glass with a TiCl₄ solution, the films were calcined using the following temperature program: heat from room temperature (rt) to 200 °C for 15 min, from 200 °C to 500 °C for 15 min, hold at 500 °C for 30 min, then cool to rt. The TiO₂ electrodes were immersed in water, methanol or 1-propanol solutions containing 0.5 mM sensitizers with/without 40, 80, or 120 mM deoxycholic acid (DCA); then, they were maintained at room temperature (rt) for 18 h. After dye loading, the films were removed and rinsed with acetonitrile. In the case of surface washing, dye-loaded TiO₂ electrodes were immersed in 1% HCl-MeOH at rt for 30 min. The dye-loaded TiO₂ electrodes were sandwiched between commercially available Pt counter electrodes (Geomatec Co., Ltd.) with electrolyte filling the gap separated by a spacer (HIMILAN: DuPont-Mitsui Polychemicals Co., Ltd.). The active area of the cells was 0.16 cm². Two types of electrolytes, iodide (I⁻/I₃⁻) and cobalt (Co²⁺/Co³⁺), were used, as they are commonly used electrolytes [35,36]. 4-*tert*-Butylpyridine (TBP) and deoxycholic acid (DCA) were occasionally added. The thicknesses of the TiO₂ films on the FTO glasses were

measured following the performance evaluation using a SURFCOM 130A (ACCRETECH Co., Ltd.). The average thickness was approximately $10 \pm 1 \mu\text{m}$.

2.5 Measurement of the cell properties

The measurement of the cell properties was performed according to a previous report [35]. The current–voltage (J–V) characteristics of the cells were measured using an AM 1.5 solar simulator (OTENTO-SUN III, Bunkoukeiki Co., Ltd.). Data were collected by a source meter (Keithley 2400), and the light-to-electricity conversion efficiency (η) was obtained according to the equation $\eta = (J_{sc} \times V_{oc} \times FF) / P_{in}$, where J_{sc} is the short-circuit photocurrent density, V_{oc} is the open-circuit voltage, FF is the fill factor, and P_{in} is the incident radiation power. The incident monochromatic photon-to-current conversion efficiency (IPCE) spectra were measured using an IPCE measurement system (SM-250 hyper mono light system, Bunkoukeiki Co., Ltd.). The IPCE values were obtained by comparing the current ratio and the IPCE value of the reference cell at each wavelength. The light intensity of the illumination source was adjusted using standard silicon photodiodes: BS520 for *J–V* characteristics and SiPD S1337-1010BQ for EQE (external quantum efficiency) measurements (Bunkoukeiki Co., Ltd.).

2.6 Computational details

The geometries of the isolated anthocyanidin dyes and dye/(TiO₂)₃₈ systems in the ground state were fully optimized by DFT calculations with the B3LYP functional [37-39]. The 6-31G basis set was used with the polarization functions for C and O atoms [40-42]. Using the optimized structures, time-dependent DFT (TD-DFT) calculations were performed to compute the absorption properties. During the TD-DFT calculations, the solvent effects were included using the conductor-like polarizable continuum model (C-PCM) [43] with the dielectric constant of

methanol. All of the calculations were performed using Gaussian 09 [44].

3. Results and discussion

3.1 Optical characteristics of anthocyanins adsorbed on TiO₂.

Nearly one thousand anthocyanins have currently been reported, and their structural variation is categorized into two parts: one is the structure of the chromophore, and the other is substitutions by sugars and organic acids, which vary by number and position. We reported that the colored seed coat of legumes contains simple anthocyanins that possess only one or two sugars at the 3-position of the chromophore. It may be better to simplify the structural variation to only the difference in the chromophore to compare the characteristics of the DSSCs using anthocyanins; thus, we chose 3-*O*-glucosides with five different chromophores, which are popular in nature. As shown in Table 1, five anthocyanins (**1-5**) in which the structural differences are only the substitution pattern of the B-ring were isolated as trifluoroacetic acid salts (TFA salts) from colored beans according to our previously reported procedure [31].

To prepare the DSSCs, all of the dyes were dissolved in MeOH (0.5 mM), and the TiO₂ electrodes were immersed in the dissolved dyes to load the pigment. Since the anthocyanins were purified as TFA salts, all of the pigments in the MeOH solutions took the flavylium cation form and presented a red color with a relatively high molecular absorptivity (ϵ) of approximately 20,000 (Table 2, Fig. S1). However, the color of the dye-loaded TiO₂ electrodes was different (Table 2, Fig. S2). The λ_{\max} values of all the dyes absorbed onto TiO₂ shifted toward longer wavelengths compared with those in 0.1% HCl-MeOH (Table 2). Pelargonidin 3-*O*-glucoside (**1**) with one OH group at the B-ring showed an orange color (λ_{\max} : 547 nm in the reflection spectrum), cyanidin 3-*O*-glucoside (**2**) with two OHs at the B-ring showed a purple color (λ_{\max} : 573 nm), delphinidin 3-*O*-glucoside (**3**) with three OHs showed a purplish blue color (λ_{\max} : 576 nm), petunidin 3-*O*-

glucoside (**4**) with two OHs and one OMe showed a blue color (λ_{max} : 580 nm), and malvidin 3-*O*-glucoside (**5**) with one OH and two OMe showed a pastel pink color (λ_{max} : 571 nm). The intensities of the cells of **2**, **3** and **4** in the reflection spectra were higher than those of **1** and **5** (Figure S2). These results indicated that anthocyanins with two or more oxygen atoms at the B-ring show deep purple (**2**), purplish blue (**3**) and blue (**4**) colors in DSSCs. This result might be due to the formation of a bond between the catechol-type B-ring and the Ti atoms in TiO₂. Upon adsorption of dyes onto TiO₂, the quinonoidal base anion form of anthocyanins might be stabilized, as was found in metal-complex anthocyanins in blue dayflower, cornflower and hydrangea [21,23-25,27-29]. Similar phenomena were reported in spectra of Pg3G (**1**), Cy3G (**2**) and Dp3G (**3**) on TiO₂ layers; specifically, they were shifted toward longer wavelengths by 10-40 nm compared to the respective ethanol solutions [45]. These results indicate that the adsorption of anthocyanin onto TiO₂ might occur at the dihydroxy group of the B-ring, not -OH at the A and C rings.

3.2 Effect of TBP on the photovoltaic properties of DSSCs using anthocyanins

With the five anthocyanin-loaded TiO₂ electrodes in hand, we fabricated DSSCs and measured their photovoltaic properties (Table 3). N719 was used as the standard dye. Since 4-*tert*-butylpyridine (TBP) was generally added to the electrolyte to increase V_{oc} [35,46,47], we first fabricated DSSCs with TBA (0.5 mM) in the electrolyte. At the same time, we compared the solvent for pigment loading. The performance of DSSCs with AM 1.5 irradiation is shown in Table 3. With TBP, the efficiencies ($\eta\%$) of the DSSCs of anthocyanins were low, ranging from 0.18-0.41%. However, without TBP, the increases in $\eta\%$ were double or more (0.56-1.11%) with the increase in J_{sc} . The addition of TBP resulted in an increase of approximately 10-20% in V_{oc} , but a decrease was observed in J_{sc} to approximately 1/4 to 1/5 compared with the absence of TBP. Combining these conflicting effects, TBP did not increase $\eta\%$ in the DSSCs of anthocyanins (Table

3, Fig. S3). It has been reported that TBP on the surface of TiO₂ decreases J_{sc} by elevating the energy level of the lower end of the conduction band of TiO₂ [46,47]. In other words, TBP causes a trade-off phenomenon between J_{sc} and V_{oc} . Our calculation results indicated that the LUMO level of anthocyanidin is near the same level of the conduction band of TiO₂; therefore, the addition of TBP might decrease the electron injection efficiency to a large extent followed by their low efficiency. The different solvents (MeOH, PrOH and acetone) during pigment loading did not produce any remarkable differences in $\eta\%$; however, among them, MeOH provided the best results, except for with Pg3G (1). Recently, a Co²⁺/Co³⁺ electrolyte showed good performance in DSSCs of porphyrins [36]; therefore, we attempted to use a Co²⁺/Co³⁺ electrolyte rather than an I⁻/I₃⁻ electrolyte. One of the reasons was that the orange color of the Co²⁺/Co³⁺ electrolyte was lighter than that of the I⁻/I₃⁻ electrolyte; thus, the cell color appeared more clear and beautiful. However, TBP is essential for using a Co²⁺/Co³⁺ electrolyte; otherwise, the performance was very low, less than 0.05% (Table S1).

3.3 Effect of DCA on the photovoltaic properties of DSSCs using anthocyanins

The chromophores of anthocyanins are well known to stack with each other [21,23-25,48]. This phenomenon is very important in stabilizing the color through inhibiting a hydration reaction [21,23-25,27]; however, this characteristic of anthocyanins might be associated with a decrease in performance. To inhibit the association of the pigments themselves, the addition of cholic acid derivatives as the coadsorbed molecule is generally utilized [49]. The addition of DCA was reported to be effective for inhibiting the self-association of anthocyanins on TiO₂ [15]. Therefore, we tested DCA with the pigment solution and fabricated DSSCs according to previous reports [35]. To the MeOH solution of each anthocyanin (0.5 mM), DCA was added with a concentration of 40 to 120 mM, and the TiO₂ electrode was immersed in the solution for 18 h at rt. After

fabrication, the performance was recorded (Table 4). The $\eta\%$ of DSSCs with Cy3G (2), Dp3G (3) and Pt3G (4) increased following the addition of DCA. The optimum concentration of DCA differed for each anthocyanin: 40 mM for both Cy3G (2) and Dp3G (3) and 80 mM for Pt3G (4) with $\eta\%$ values of 1.09%, 1.22% and 1.42%, respectively (Table 4, Fig. 1, 2). In contrast, Pg3G (1) and Mv3G (5) did not show such an increase in $\eta\%$, with values of 0.51% and 0.56%, respectively. In general, the effect of DCA is thought to decrease the molecular association of dyes that causes intermolecular energy quenching [49]. Regarding Cy3G (2), Dp3G (3) and Pt3G (4), the amounts of absorbed dye might be higher than those of Pg3G and Mv3G (indicated by the color density, Table 2); therefore, the addition of DCA may effectively decrease the molecular stacking and then provide an increase in efficiency [49]. The J_{sc} values of the former three anthocyanins (2-4) were approximately 6 mA/cm², and those of the latter two (1 and 5) were less than 3 mA/cm². The V_{oc} values of these were approximately 350 mV without any significant differences; therefore, the good efficiencies of 2-4 should be due to the increase in the J_{sc} values (Fig. 1). The IPCE spectra of the DSSCs of the anthocyanins are shown in Fig. 2. Compared with the spectra of high-performance dyes such as N719 and black dye, the IPCE spectra of anthocyanins are low, below 50% from 400-800 nm. Among them, Cy3G (2) showed relatively high peaks at approximately 600 nm. The IPCE spectra of the DSSCs (Fig. 2) showed shapes similar to those observed in the reflection spectra (Fig. S2). This phenomenon is observed when direct electron transfer occurs [50]; therefore, the observed characteristics indicate that direct electron transfer might occur to some extent in the electron injection mechanisms of DSSCs fabricated with anthocyanins.

Since the addition of DCA provided a good result in DSSCs of anthocyanins, the property of anthocyanins being easy to stack with each other might produce a negative effect on efficiency. Compared with metal complex dyes such as N719 and black dye, the adsorption of anthocyanins on

TiO₂ appeared to be faster because the usual loading period of N719 is 18 h, but that of anthocyanin of 3 h and 18 h did not result in significant differences. Finally, we tested the effect of surface washing of the dye-loaded electrode with 1% HCl-MeOH for 30 min. As shown in Table 4, the effect was observed only in the DSSCs of Cy3G, with an increase in the $\eta\%$ from 1.09% to 1.25% (Table 4). The other anthocyanins did not show such an increase in $\eta\%$ as a result of washing.

3.4 Effect of the glucoside of anthocyanins on their photovoltaic properties

In nature, all anthocyanins are found as glycosylated compounds, and the existence of a chiral sugar exhibits a large effect on the molecular stacking structure of anthocyanins [51]. Therefore, to clarify the effect of the sugar, the aglycone of anthocyanin, anthocyanidin, was prepared by acid hydrolysis and used in the fabricated DSSCs. We attempted to use cyanidin (6) and petunidin (7) because of the high performance of Cy3G (2) and Pt3G (4). The efficiencies of these without TBP and DCA were 0.55% and 0.69%, respectively, and the addition of DCA (40 mM) increased the $\eta\%$ to 0.94% and 0.79% (Table 5). However, the values of the aglycones were lower than those of glucosides, indicating that the presence of the sugar at the 3-position should positively influence the performance of DSSCs. The effect of 3-*O*-glycosylation might be due to the inhibition of the self-association of chromophores; the chemical mechanism of this should be resolved in the future.

3.5 DFT and TD-DFT calculations for anthocyanidin dyes and dye/(TiO₂)₃₈ systems

We started the theoretical calculations by determining the geometries of the anthocyanidin dyes and the dye/(TiO₂)₃₈ systems. For the isolated dyes, the flavylum ion form was considered for comparison with the observed absorptions. The dyes have nearly planar structures, and their geometry optimizations are easy. Those for the dye/(TiO₂)₃₈ systems,

however, are not easy because many local minima are expected for these systems. Thus, their geometry optimizations were conducted with a few assumptions, as follows. By considering that a bridging bidentate structure in the quinonoidal form was computed to be stable in the cyanidin-TiO₂ nanowire system [32,33], the cyanidin/(TiO₂)₃₈ system was optimized from such a structure. The obtained optimized structure is shown in Fig. 3, where two O atoms and one H atom in the B-ring bond to the five-coordinated Ti and two-coordinated O atoms in the semiconductor, respectively. Note that the experimental results shown above also imply that the adsorption occurs through the B-ring, with the dyes being in the quinonoidal base anion form. Starting from the structure derived from the optimized cyanidin/(TiO₂)₃₈ structure by introducing substituents, the geometry optimizations were conducted for delphinidin/(TiO₂)₃₈ and petunidin/(TiO₂)₃₈. Because malvidin and pelargonidin have only one hydroxy group in the B-ring, the monodentate structures were assumed for malvidin/(TiO₂)₃₈ and pelargonidin/(TiO₂)₃₈, where the quinonoidal form was again considered for the anthocyanidins. Note that examining various adsorption structures is beyond the scope of this study.

Table 6 summarizes the excitation energies and their assignments for cyanidin (**6**), pelargonidin (**8**), and their dye/(TiO₂)₃₈ systems calculated at the determined structures. As shown in Table 6, the first peak maxima correspond to the transitions from the highest occupied molecular orbital (HOMO) to the lowest unoccupied molecular orbital (LUMO) and are located at 490 and 478 nm for cyanidin and pelargonidin, respectively. These values reasonably agree with the experimental results of 530 and 510 nm shown in Table 2. By contrast, for the dye/(TiO₂)₃₈ systems, the absorption peaks with non-negligible oscillator strengths appear at longer wavelength regions, ~514-566 nm and ~505-518 nm for cyanidin and pelargonidin, respectively. These results are qualitatively consistent with the experimental observations as argued above and support the present model systems. Note that similar arguments hold for other three dye systems, as shown in

Table S2.

The optical properties can be clarified by examining the characteristics of the Kohn-Sham orbitals and the excited states for the dye/(TiO₂)₃₈ clusters. Table 7 summarizes some orbital energies and the weights of the dye atomic orbitals for cyanidin/(TiO₂)₃₈ and pelargonidin/(TiO₂)₃₈. The results for the other three dye systems are summarized in Table S3. As shown in Table 7, the HOMOs for these cluster systems are dominated by the dye atomic orbitals and assigned to the dye HOMOs, whereas the contributions of the semiconductor atomic orbitals are large for the low-lying unoccupied orbitals. For example, the orbitals from LUMO+2 to LUMO+6 for cyanidin/(TiO₂)₃₈ are mainly composed of the semiconductor atomic orbitals, as shown in Table 7. Consistently, the second, fourth, and fifth excited states, which are mainly assigned to the transitions from the HOMO to these orbitals, have very small oscillator strengths, as shown in Table 6. By contrast, the LUMO and the LUMO+1 are delocalized between the cyanidin and semiconductor: 40% and 37% of these orbitals originate from the cyanidin atomic orbitals (Table 7). Because the first and third excited states are mainly assigned to the transitions to these orbitals, the relatively large oscillator strengths of 0.2819 and 0.3903, respectively, are rationalized. In addition, the delocalized nature of these orbitals indicates that the computed absorptions at 566 and 547 nm for cyanidin/(TiO₂)₃₈ have characteristics of direct charge transfer excitation to some extent, which is consistent with the above experimental argument. Although the sixth excited state is mainly assigned to the transition to the semiconductor orbital (LUMO+4), its oscillator strength of 0.1738 is not negligible. However, this can be explained on the basis of the natural transition orbital (NTO) pairs [52]. As shown in Fig. 4(a), the non-negligible oscillator strength for the sixth excited state is attributed to the delocalization between the dye and the semiconductor in the particle. It was found that the same argument holds for the low-lying excited states for delphinidin/(TiO₂)₃₈ and petunidin/(TiO₂)₃₈.

For pelargonidin/(TiO₂)₃₈, although both the second and third excited states are assigned to the transitions involving LUMO+1 and LUMO+2, the oscillator strengths of 0.8510 and 0.0024 for these two states are completely different. This difference can again be explained on the basis of the NTOs shown in Figs. 4(c) and 4(d). The second excited state is largely characterized by the transition within the dye (Fig. 4(c)); hence, the large oscillator strength is rationalized. The nearly zero oscillator strength of the third excited state is attributed to the completely different character of the particle (Fig. 4(d)). The relatively large oscillator strength of 0.2646 for the first excited state is attributed to the delocalization between the dye and semiconductor in the particle (Fig. 4(b)). These results imply that both the direct (Type II) and indirect (Type I) charge transfer mechanisms might co-exist for pelargonidin/(TiO₂)₃₈. It was also found that the same argument holds for malvidin/(TiO₂)₃₈.

Finally, note that the transition within the dye observed for pelargonidin/(TiO₂)₃₈ and malvidin/(TiO₂)₃₈ might be attributed to the monodentate adsorption because only single bonding between Ti and O in the B-ring implies a weaker coupling. However, care must be taken because all possible adsorption structures, including monodentate ones, were not investigated for the cyanidin, delphinidin, and petunidin model systems in this study. In addition, the energy relationship between the dye LUMO and the conduction band might be changed by details of the environment, such as adsorption structures and solvent effects, which might modify the transition mechanism, even qualitatively. In fact, in the calculations without solvent effects for all five of the dye/(TiO₂)₃₈ clusters, it was found that the LUMOs are characterized by the dyes and lower in energy than the conduction band. Note that the cyanidin LUMO was found to be slightly lower in energy than the conduction band minimum in the previous first-principles calculations for the TiO₂ nanowire system [32,33,53]. In these respects, more elaborate investigations including various adsorption structures would be valuable for obtaining deeper insights into anthocyanin

DSSC systems.

4. Conclusion

In conclusion, we prepared DSSCs using five pure anthocyanidin 3-*O*-glucosides and two anthocyanidins and then analyzed their photovoltaic properties. The color of the DSSC of Pg3G (**1**) was orange, that of Mv3G (**5**) was purple, and those of Cy3G (**2**), Dp3G (**3**) and Pt3G (**4**) were blue. To immerse TiO₂, MeOH provided the best result as a solvent in almost all of the anthocyanins except Pg3G; PrOH resulted in the best η° . The addition of TBP (0.5 mM) decreased the η° value for all of the anthocyanins. In contrast, the addition of DCA (40-80 mM) increased the η° of the DSSCs of Cy3G (**2**), Dp3G (**3**) and Pt3G (**4**). The J_{sc} values of the DSSCs of Cy3G (**2**), Dp3G (**3**) and Pt3G (**4**) were approximately 5 mA/cm², and the V_{oc} values were approximately 350 mV. The conversion efficiency (η°) of these under the optimized conditions were approximately 0.6-1.4%. The highest η° value was obtained from the DSSC of Pt3G at 1.42% (Table 4). The TD-DFT calculations for the anthocyanidin dye model cluster systems, dye/(TiO₂)₃₈, revealed that both indirect (Type-I) and direct (Type-II) electron injection mechanisms might co-exist.

Acknowledgements

We are grateful to Prof. Segawa and Prof. Uchida of The University of Tokyo and Prof. Kondo and Prof. Kajiwara of Nagoya University for their suggestions and fruitful discussions. This work was supported by a JSPS KAKENHI, Grant-in-Aid for Exploratory Research (No. 24651091) and the Collaborative Research Program of Institute for Chemical Research, Kyoto University (grant #2013-37, #2014-40, #2015-53 and #2016-48). The computations were primarily performed using facilities of the Information Technology Center, Nagoya University.

References

- [1] B. O'Regan, M. Grätzel, A low-cost, high-efficiency solar cell based on dye-sensitized colloidal TiO₂ films, *Nature* 353 (1991) 737-740.
- [2] M. K. Nazeerddin, A. Kay, I. Rodicio, R. Humphry-Baker, E. Müller, P. Liska, N. Vlachopoulos, M. Grätzel, Conversion of Light to Electricity by cis-X₂Bis(2,2'-bipyridyl-4,4'-dicarboxylate) ruthenium (II) Charge-Transfer Sensitizers (X = Cl⁻, Br⁻, I⁻, CN⁻, and SCN⁻) on Nanocrystalline TiO₂ Electrodes, *J. Am. Chem. Soc.* 115 (1993) 6382-6390.
- [3] K. Kakiage, Y. Aoyama, T. Yano, K. Oya, J. Fujisawa, M. Hanaya, Highly-efficient dye-sensitized solar cells with collaborative sensitization by silyl-anchor and carboxy-anchor dyes, *Chem. Commun.* 51 (2015) 15894-15897.
- [4] T. Toyoda, T. Sano, J. Nakajima, S. Doi, S. Fukumoto, A. Ito, T. Yohyama, M. Yoshida, T. Kanagawa, T. Motohiro, T. Shiga, K. Higuchi, H. Tanaka, Y. Takeda, T. Fukano, N. Katoh, A. Takeichi, K. Takechi, M. Shiozawa, Outdoor performance of large scale DSC modules, *J. Photochem. Photobiol. A* 164 (2004) 203-207.
- [5] J. B. Baxter, Commercialization of dye sensitized solar cells: Present status and future research needs to improve efficiency, stability, and manufacturing, *J. Vac. Sci. Technol. A* 30 (2012) 020801-1-19.
- [6] S. Essig, S. Ward, M. A. Steiner, D. J. Friedman, J. F. Geisz, P. Stradins, D. L. Young, Progress towards a 30% efficient GaInP/Si tandem solar cell, *Energy Procedia* 77 (2015) 464-469.
- [7] A. Kojima, K. Teshima, Y. Shirai, T. Miyasaka, Organometal Halide Perovskites as Visible-Light Sensitizers for Photovoltaic Cells, *J. Am. Chem. Soc.* 131 (2009) 6050-6051.
- [8] W. S. Yang, J. H. Noh, N. J. Jeon, Y. C. Kim, S. Ryu, J. Seo, S. I. Seok, High-performance photovoltaic perovskite layers fabricated through intramolecular exchange, *Science* 348

(2015) 1234-1237.

- [9] A. Hagfeldt, G. Boschloo, L. Kloo, H. Pettersson, Dye-Sensitized Solar Cells, *Chem. Rev.* 110 (2010) 6595-6663.
- [10] G. Calogero, A. Bartolotta, G. D. Marco, A. D. Carlo, F. Bonaccorso, Vegetable-based dye-sensitized solar cells, *Chem. Soc. Rev.* 44 (2015) 3244-3294.
- [11] K. Tennakone, G. R. R. A. Kumara, A. R. Kumarasighe, K. G. U. Wijayantha, P. M. Sirimanne, A dye-sensitized nano-porous I solid-state photovoltaic cell, *Semicond. Sci. Technol.* 10 (1995) 1689-1693.
- [12] N. J. Cherepy, G. P. Smestad, M. Grätzel, J. Z. Zhang, Ultrafast Electron Injection: Implications for a Photoelectrochemical Cell Utilizing an Anthocyanin Dye-Sensitized TiO₂ Nanocrystalline Electrode, *J. Phys. Chem. B* 101 (1997) 9342-9351.
- [13] W. H. Lai, Y. H. Su, L. G. Teoh, M. H. Hon, Commercial and natural dyes as photosensitizers for a water-based dye-sensitized solar cell loaded with gold nanoparticles, *J. Photochem. Photobiol. A* 195 (2008) 307-313.
- [14] G. Calogero, J-H. Yum, A. Sinopoli, G. D. Marco, M. Grätzel, M. K. Nazeeruddin, Anthocyanins and betalains as light-harvesting pigments for dye-sensitized solar cells, *Solar Energy*, 86 (2012) 1563-1575.
- [15] C-Y. Chien, B-D. Hsu, Optimization of the dye-sensitized solar cell with anthocyanin as photosensitizer, *Solar Energy*, 98 (2013) 203-211.
- [16] Y. Li, S-H. Ku, S-M. Chen, M. A. Ali, F. A. M. AlHemaid, Photoelectrochemistry for Red Cabbage Extract as Natural Dye to Develop a Dye-Sensitized Solar Cells, *Int. J. Electrochem. Sci.* 8 (2013) 1237-1245.
- [17] S. Shalini, R. B. Prabhu, S. Prasanna, T. K. Mallick, S. Senthilarasu, Review on natural dye sensitized solar cells: Operation, materials and methods, *Renewable and Sustainable Energy*

Reviews 51 (2015) 1306-1325.

- [18] F. Teoli, S. Lucioli, P. Nota, A. Frattarelli, F. Matteocci, A. D. Carlo, E. Caboni, C. Forni, Role of pH and pigment concentration for natural dye-sensitized solar cells treated with anthocyanin extracts of common fruits, *J. Photochem. Photobiol. A* 316 (2016) 24-30.
- [19] N.A. Treat, F. J. Knorr, J. L. McHale, Templated Assembly of Betanin Chromophore on TiO₂: Aggregation-Enhanced Light-Harvesting and Efficient Electron Injection in a Natural Dye-Sensitized Solar Cell, *J. Phys. Chem. C* 120 (2016) 9122-9131.
- [20] P. Chaiamornnugool, S. Tontapha, R. Phatchana, N. Ratchapolthavisin, S. Kanokmedhakul, W. Sang-aroon, V. Amornkitbamrung, Performance and stability of low-cost dye-sensitized solar cell based crude and pre-concentrated anthocyanins: Combined experimental and DFT/TDDFT study, *J. Mol. Struct.* 1127 (2017) 145-155.
- [21] T. Goto, T. Kondo, Structure and Molecular Stacking of Anthocyanins Flower Color Variation, *Angew. Chem. Int. Ed. Engl.* 30 (1991) 17-33.
- [22] D. Strack, V. Wray, The Anthocyanins, in: J. B. Harborne (Eds.), *The Flavonoids Advances in Research science* 1986, Chapman & Hall, London, 1994, pp. 1-19.
- [23] R. Brouillard, O. Dangles, Flavonoids and Flower colour, in: J. B. Harborne (Eds.), *The Flavonoids Advances in Research science* 1986, Chapman & Hall, London, 1994, pp. 569-586.
- [24] O. M. Andersen, M. Jordheim, The Anthocyanins, in: O. M. Andersen, K. R. Markham (Eds.), *Flavonoids, Chemistry, Biochemistry and applications*, CPC Press, Boca Raton, 2006, pp. 471-551.
- [25] K. Yoshida, M. Mori, T. Kondo, Blue flower color development by anthocyanins: from chemical structure to cell physiology, *Nat. Prod. Rep.* 26 (2009) 884-915.
- [26] R. Brouillard, B. Delaporte, *Chemistry of Anthocyanin Pigments. 2. Kinetic and Thermodynamic Study of Proton Transfer, Hydration, and Tautomeric Reactions of Malvidin*

- 3-Glucoside, *J. Am. Chem. Soc.* 99 (1977) 8461-8468.
- [27] T. Kondo, K. Yoshida, A. Nakagawa, T. Kawai, H. Tamura, T. Goto, Structural Basis of Blue-colour development in flower petals: structure determination of commelinin from *Commelina communis*, *Nature* 358 (1992) 515-518.
- [28] T. Kondo, M. Ueda, H. Tamura, K. Yoshida, M. Isobe, T. Goto, Composition of protocyanin, a self-assembled supramolecular pigment from the blue cornflower *Centaurea cyanus*, *Angew. Chem. Int. Ed. Engl.* 33 (1994) 978-979.
- [29] K-I. Oyama, T. Yamada, D. Ito, T. Kondo, K. Yoshida, Metal-complex pigment involved in the blue sepal color development of hydrangea, *J. Agric. Food. Chem.* 63 (2015) 7630-7635.
- [30] G. Calogero, A. Sinopoli, I. Citro, C. D. Marco, V. Petrov, A. M. Diniz, A. J. Parola, F. Pina, Synthetic analogues of anthocyanins as sensitizers for dye-sensitized solar cells, *Photochem Photobiol Sci.* 148 (2013) 883-894.
- [31] K. Yoshida, Y. Sato, R. Okuno, K. Kameda, M. Isobe, T. Kondo, Structural Analysis and Measurement of Anthocyanins from Colored Seed Coats of *Vigna*, *Phaseolus*, and *Glycine* Legumes, *Biosci. Biotech. Biochem.* 60 (1996) 589-593.
- [32] S. Meng, J. Ren, E. Kaxiras, Natural Dyes Adsorbed on TiO₂ Nanowire for Photovoltaic Applications: Enhanced Light Absorption and Ultrafast Electron Injection, *Nano Lett.* 8 (2008) 3266–3272.
- [33] Y. Jiao, Z. Ding, S. Meng, Atomistic mechanism of charge separation upon photoexcitation at the dye-semiconductor interface for photovoltaic applications, *Phys. Chem. Chem. Phys.* 13 (2011) 13196-13201
- [34] S. Agrawal, M. Pastore, G. Marotta, M. A. Reddy, M. Chandrasekharam, F. De Angelis, Optical Properties and Aggregation of Phenothiazine-Based Dye-Sensitizers for Solar Cells Applications: A Combined Experimental and Computational Investigation, *J. Phys. Chem. C*

117 (2013) 9613–9622.

- [35] Y. Liu, H. Lin, K. Tamaki, J. Nakazaki, C. Nishiyama, S. Uchida, H. Segawa, J. Li, Kinetics versus Energetics in Dye-Sensitized Solar Cells Based on an Ethynyl-Linked Porphyrin Heterodimer, *J. Phys. Chem. C* 118 (2014) 1426-1435.
- [36] A. Yella, H-W. Lee, H. N. Tsao, C. Yi, A. K. Chandiran, M. Nazeeruddin, E. W-G. Diao, C-Y. Yeh, S. M. Zakeeruddin, M. Grätzel, Porphyrin-Sensitized Solar Cells with Cobalt (II/III)-Based Redox Electrolyte Exceed 12 Percent Efficiency, *Science*, 334 (2011) 629-634.
- [37] C. Lee, W. Yang, R. G. Parr, Development of the Colle-Salvetti correlation-energy formula into a functional of the electron density, *Phys. Rev. B* 37 (1988) 785-789.
- [38] B. Miehlich, A. Savin, H. Stoll, H. Preuss, Results obtained with the correlation energy density functionals of Becke and Lee, Yang and Parr, *Chem. Phys. Lett.* 157 (1989) 200-206.
- [39] A. D. Becke, Density-functional thermochemistry. III. The role of exact exchange, *J. Chem. Phys.* 98 (1993) 5648-5652.
- [40] W. J. Hehre, R. Ditchfield, J. A. Pople, Self-Consistent Molecular Orbital Methods. XII. Further Extensions of Gaussian-Type Basis Sets for Use in Molecular Orbital Studies of Organic Molecules, *J. Chem. Phys.* 56 (1972) 2257-2261.
- [41] P. C. Hariharan, J. A. Pople, The Influence of Polarization Functions on Molecular Orbital Hydrogenation Energies, *Theoret. Chim. Acta* 28 (1973) 213-222.
- [42] V. A. Rassolov, J. A. Pople, M. A. Ratner, T. L. Windus, 6-31G* basis set for atoms K through Zn, *J. Chem. Phys.* 109 (1998) 1223-1229.
- [43] M. Cossi, N. Rega, G. Scalmani, V. Barone, Energies, Structures, and Electronic Properties of Molecules in Solution with the C-PCM Solvation Model, *J. Comp. Chem.* 24 (2003) 669-681.
- [44] Gaussian 09, Revision E.01, M. J. Frisch, G. W. Trucks, H. B. Schlegel, G. E. Scuseria, M. A. Robb, J. R. Cheeseman, G. Scalmani, V. Barone, B. Mennucci, G. A. Petersson, H. Nakatsuji,

M. Caricato, X. Li, H. P. Hratchian, A. F. Izmaylov, J. Bloino, G. Zheng, J. L. Sonnenberg, M. Hada, M. Ehara, K. Toyota, R. Fukuda, J. Hasegawa, M. Ishida, T. Nakajima, Y. Honda, O. Kitao, H. Nakai, T. Vreven, J. A. Montgomery, Jr., J. E. Peralta, F. Ogliaro, M. Bearpark, J. J. Heyd, E. Brothers, K. N. Kudin, V. N. Staroverov, R. Kobayashi, J. Normand, K. Raghavachari, A. Rendell, J. C. Burant, S. S. Iyengar, J. Tomasi, M. Cossi, N. Rega, J. M. Millam, M. Klene, J. E. Knox, J. B. Cross, V. Bakken, C. Adamo, J. Jaramillo, R. Gomperts, R. E. Stratmann, O. Yazyev, A. J. Austin, R. Cammi, C. Pomelli, J. W. Ochterski, R. L. Martin, K. Morokuma, V. G. Zakrzewski, G. A. Voth, P. Salvador, J. J. Dannenberg, S. Dapprich, A. D. Daniels, Ö. Farkas, J. B. Foresman, J. V. Ortiz, J. Cioslowski, D. J. Fox, Gaussian, Inc., Wallingford CT (2009).

[45] Q. Dai, J. Rabani, Photosensitization of nanocrystalline TiO₂ films by anthocyanin dyes, *J Photochem. Photobiol. A* 148 (2002) 17-24.

[46] S. Y. Huang, G. Schlichthörl, A. J. Nozik, M. Grätzel, Frank, A. J. Charge Recombination in Dye-Sensitized Nanocrystalline TiO₂ Solar Cells. *J. Phys. Chem. B* 101 (1997) 2576-2582.

[47] K. Zhang, S. Zhang, K. Sodeyama, X. Yang, H. Chen, M. Yanagida, Y. Tateyama, L. A. Han, A New Factor Affecting the Performance of Dye-Sensitized Solar Cells in the Presence of 4-*tert*-Butylpyridine, *Appl. Phys. Express* 5 (2012) 1-3.

[48] Y. Leydet, R. Gavara, V. Petrov, A. M. Diniz, A. J. Parola, J. C. Lima, F. Pina, The effect of self-aggregation on the determination of the kinetic and thermodynamic constants of the network of chemical reactions in 3-glucoside anthocyanins, *Phytochemistry* 83 (2012) 125-135.

[49] A. Kay, M. Grätzel, Artificial Photosynthesis. 1. Photosensitization of TiO₂ Solar Cells with Chlorophyll Derivatives and Related Natural Porphyrins, *J. Phys. Chem.* 97 (1993) 6272-6277.

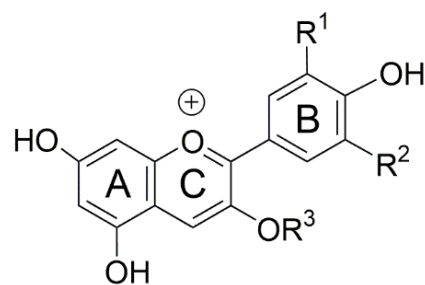
[50] M. Tae, S. H. Lee, J. K. Lee, S. S. Yoo, E. J. Kang, K. B. Yoon, A Strategy To Increase the Efficiency of the Dye-Sensitized TiO₂ Solar Cells Operated by Photoexcitation of Dye-to-TiO₂

Charge-Transfer Bands, *J. Phys. Chem. B* 109 (2005) 22513-22522.

- [51] T. Kondo, K-I. Oyama, K. Yoshida, Chiral Molecular Recognition on Formation of a Metalloanthocyanin: A Supramolecular Metal Complex Pigment from Blue Flowers of *Salvia patens*, *Angew. Chem. Int. Ed.* 40 (2001) 894-897.
- [52] R. L. Martin, Natural transition orbitals, *J. Chem. Phys.* 118 (2003) 4775-4777.
- [53] H. Ünal, D. Gunceler, O. Gülseren, Ş. Ellialtıođlu, E. Mete, Anatase TiO₂ nanowires functionalized by organic sensitizers for solar cells: A screened Coulomb hybrid density functional study, *J. Appl. Phys.* 118 (2015) 194301-1-10.
- [54] N. M. O'Boyle, A. L. Tenderholt, K. M. Langner, cclib: A Library for Package-Independent Computational Chemistry Algorithms, *J. Comp. Chem.* 29 (2008) 839-845.

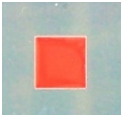
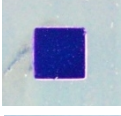
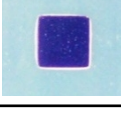
Table 1

Structures of anthocyanins and anthocyanidins studied for DSSCs.



	R ¹	R ²	R ³	anthocyanin	aglycone
Pg3G (1)	H	H	Glc	pelargonin	pelargonidin
Cy3G (2)	OH	H	Glc	cyanin	cyanidin
Dp3G (3)	OH	OH	Glc	delphin	delphinidin
Pt3G (4)	OCH ₃	OH	Glc	petunin	petunidin
Mv3G (5)	OCH ₃	OCH ₃	Glc	malvin	malvidin
Cy (6)	OH	H	H	—	cyanidin
Pt (7)	OH	H	H	—	petunidin
Pg (8)	H	H	H	—	pelargonidin

Table 2Optical properties of the dyes (**1-7**) and photographs of the dye-adsorbed TiO₂ electrodes.

Dye	UV-Vis ^a	Reflectance ^b	Dye-adsorbed TiO ₂ electrodes
	$\lambda_{\text{max}}/\text{nm}$ ($\epsilon \text{ M}^{-1}\text{cm}^{-1}$)	$\lambda_{\text{max}}/\text{nm}$ (shift value)	
Pg3G (1)	510 (15,700)	547 (37)	
Cy3G (2)	530 (19,600)	573 (43)	
Dp3G (3)	541 (23,800)	576 (35)	
Pt3G (4)	540 (24,300)	580 (40)	
Mv3G (5)	539 (12,400)	571 (32)	
Cy (6)	541 (20,800)	562 (21)	
Pt (7)	547 (22,600)	572 (25)	

^a TFA-salts of dyes were dissolved in MeOH (0.5 mM), and UV-vis spectra (path length: 10 mm) were recorded.

^b Reflection spectra of dye-adsorbed TiO₂ electrodes were recorded using an integrating sphere.

Table 3

Photovoltaic properties of the DSSCs sensitized with anthocyanins (**1-5**) in terms of the difference in immersing solvent and existence of TBP^a.

Dye	Solvent ^b	TBP ^c (0.5 mM)	J_{sc} (mA/cm ²)	V_{oc} (mV)	FF	η (%)
Pg3G (1)	MeOH	(+)	0.63	440	0.64	0.18
		(-)	2.68	377	0.56	0.56
	PrOH	(-)	3.55	343	0.60	0.73
Cy3G (2)	MeOH	(+)	1.29	434	0.69	0.39
		(-)	4.93	355	0.61	1.06
	PrOH	(-)	4.56	327	0.59	0.88
	Acetone	(-)	5.86	322	0.51	0.97
Dp3G (3)	MeOH	(+)	0.85	407	0.66	0.23
		(-)	5.22	354	0.59	1.08
	PrOH	(-)	4.02	337	0.57	0.77
	Acetone	(-)	5.52	328	0.51	0.92
Pt3G (4)	MeOH	(+)	1.37	420	0.71	0.41
		(-)	4.93	385	0.58	1.11
	PrOH	(-)	4.37	339	0.6	0.89
	Acetone	(-)	5.44	331	0.54	0.97
Mv3G (5)	MeOH	(+)	0.88	468	0.70	0.29
		(-)	3.25	343	0.58	0.64
	PrOH	(-)	2.79	332	0.62	0.58
N719	Acetonitrile/ tert-butanol =1:1	(+)	15.7	717	0.64	7.3

^a For measurement of photovoltaic properties, I⁻/I₃⁻ was used as an electrolyte.

^b Dyes were dissolved in each solvent with a concentration of 0.5 mM and immersed at rt for 18 h.

^c TBP was added to the electrolyte.

Table 4Effect of DCA on the photovoltaic properties of the DSSCs sensitized with anthocyanins (**1-5**)^a.

Dye ^b	DCA (mM)	Surface washing ^c	J_{sc} (mA/cm ²)	V_{oc} (mV)	FF	η (%)
Pg3G (1)	80	(-)	2.57	375	0.53	0.51
Cy3G (2)	40	(-)	5.15	352	0.60	1.09
	40	(+)	6.59	347	0.55	1.25
	80	(-)	5.07	359	0.59	1.08
	120	(-)	5.80	348	0.53	1.06
Dp3G (3)	40	(-)	5.96	348	0.59	1.22
	80	(-)	5.86	358	0.55	1.15
	120	(-)	7.28	319	0.49	1.14
Pt3G (4)	40	(-)	6.59	348	0.59	1.36
	80	(-)	6.32	360	0.62	1.42
	120	(-)	6.72	338	0.52	1.18
Mv3G (5)	80	(-)	2.70	326	0.63	0.56

^a For measurement of photovoltaic properties, I⁻/I₃⁻ was used as an electrolyte.^b Dyes were dissolved in MeOH with a concentration of 0.5 mM and immersed at rt for 18 h.^c Surface washing was performed with 1% HCl-MeOH at rt for 30 min.

Table 5Photovoltaic properties of the DSSCs sensitized with anthocyanidins (**6**, **7**)^a.

Dye ^b	DCA (mM)	J_{sc} (mA/cm ²)	V_{oc} (mV)	FF	η (%)
Cy (6)	(-)	3.17	352	0.49	0.55
	40	4.30	360	0.61	0.94
Pt (7)	(-)	3.95	304	0.57	0.69
	40	4.61	310	0.56	0.79

^a For measurement of photovoltaic properties, I⁻/I₃⁻ was used as an electrolyte.^b Dyes were dissolved in MeOH with a concentration of 0.5 mM and immersed at rt for 18 h.

Table 6

Absorption energies (eV), oscillator strengths f , and transition characteristic of the singlet excited states of the cyanidin, pelargonidin and dye/(TiO₂)₃₈ systems.

state	energy ^a	f	assignment ^b
cyanidin (6)			
1	2.53 (490)	0.5972	H→L (93%)
cyanidin/(TiO₂)₃₈			
1	2.19 (566)	0.2819	H→L (70%)
2	2.22 (557)	0.0525	H→L+2 (87%)
3	2.27 (547)	0.3903	H→L+1 (80%)
4	2.32 (535)	0.0176	H→L+3 (57%)
5	2.36 (525)	0.0620	H→L+5 (31%), H→L+6 (21%)
6	2.41 (514)	0.1738	H→L+4 (61%)
pelargonidin (8)			
1	2.59 (478)	0.5404	H→L (90%)
pelargonidin/(TiO₂)₃₈			
1	2.39 (518)	0.2646	H→L (86%)
2	2.46 (505)	0.8510	H→L+1 (42%), H→L+2 (51%)
3	2.51 (493)	0.0024	H→L+1 (50%), H→L+2 (35%)

^a Values in nm are given in parentheses.

^b Contributions above 20% are presented. H and L represent HOMO and LUMO, respectively.

Table 7

Orbital energies ε (eV) and contributions (%) of the dye atomic orbitals for cyanidin/(TiO₂)₃₈ and pelargonidin/(TiO₂)₃₈ with C-PCM.

Orbital	ε (eV)	weight (%) ^a
cyanidin/(TiO ₂) ₃₈		
LUMO+6	-2.86	1
LUMO+5	-2.90	3
LUMO+4	-2.91	6
LUMO+3	-2.95	1
LUMO+2	-3.04	0
LUMO+1	-3.10	37
LUMO	-3.12	40
HOMO	-5.64	95
pelargonidin/(TiO ₂) ₃₈		
LUMO+6	-2.86	0
LUMO+5	-2.91	0
LUMO+4	-2.91	1
LUMO+3	-2.99	2
LUMO+2	-3.08	27
LUMO+1	-3.10	43
LUMO	-3.14	18
HOMO	-5.83	98

^a Calculated using GaussSum program [54].

Figure Legends:

- Fig. 1.** Current-voltage curves of the DSSCs sensitized with anthocyanins (**1-5**) under the optimized conditions.
- Fig. 2.** IPCE spectra of the DSSCs sensitized with anthocyanins (**1-5**) under the optimized conditions.
- Fig. 3.** Optimized structure of the cyanidin/(TiO₂)₃₈ system. Two O atoms in the B-ring bond to the five-coordinated Ti (Ti5c). The proton dissociated from the B-ring is adsorbed onto the two-coordinated O (O2c) in the semiconductor.
- Fig. 4.** Natural transition orbitals for (a) the sixth excited state of cyanidin/(TiO₂)₃₈, and (b) the first, (c) second, and (d) third excited states of pelargonidin/(TiO₂)₃₈. The hole (left) and particle (right) are shown, where the eigenvalues of these pairs are larger than 0.98, and thus, the transitions are characterized by one single pair.

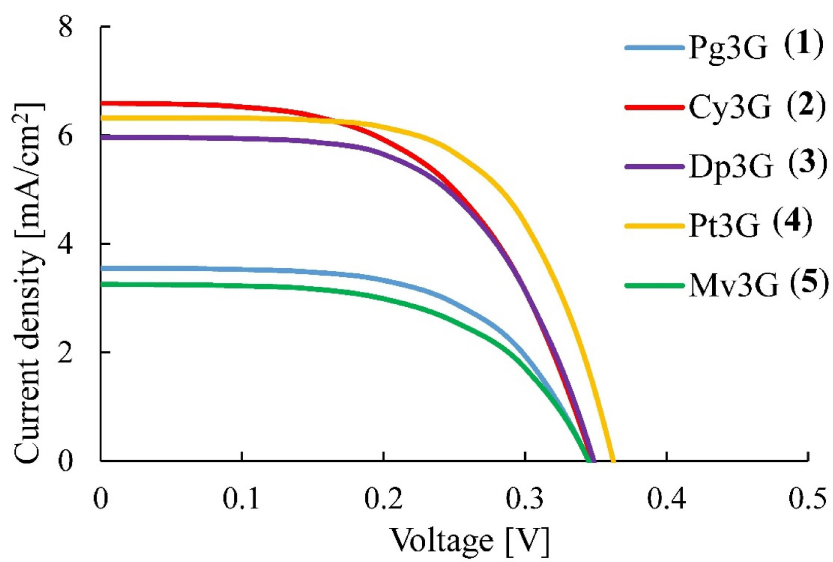


Fig. 1. Current-voltage curves of the DSSCs sensitized with anthocyanins (1-5) under the optimized conditions.

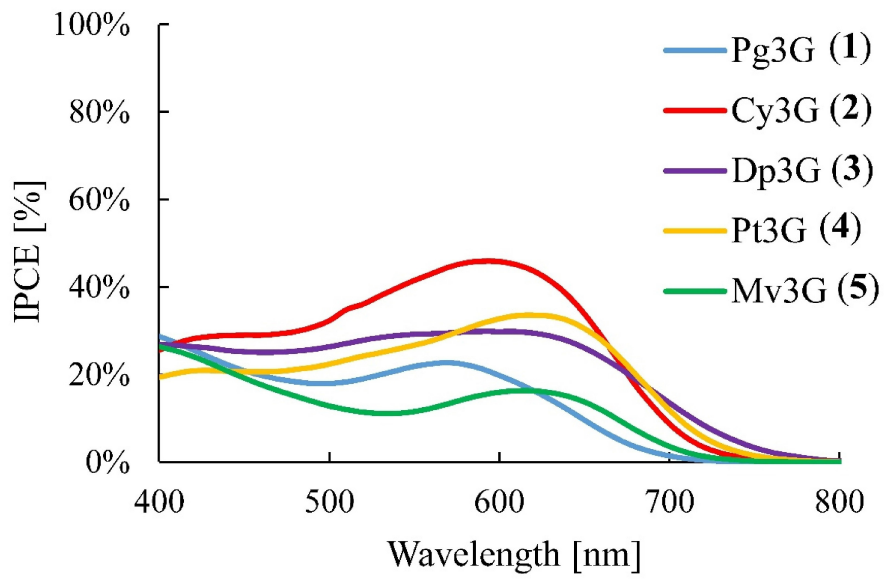


Fig. 2. IPCE spectra of the DSSCs sensitized with anthocyanins (1-5) under the optimized conditions.

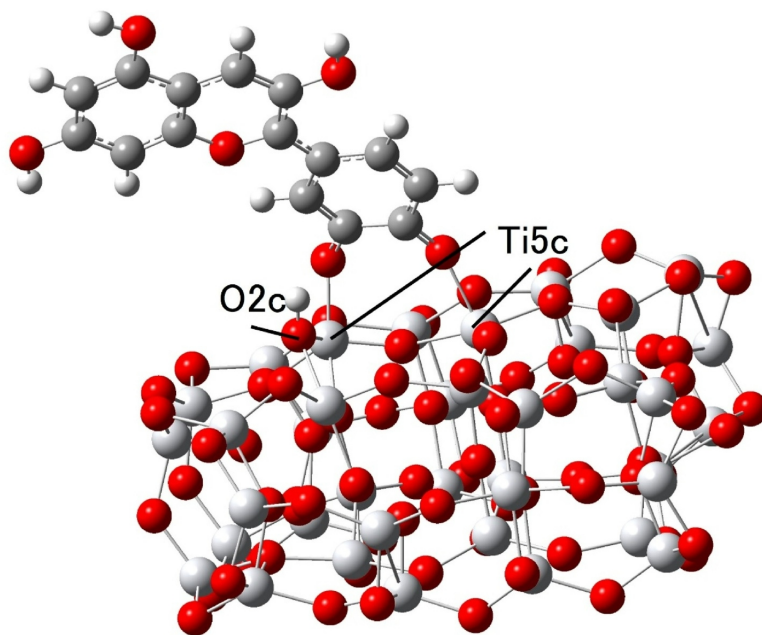


Fig. 3. Optimized structure of the cyanidin/ $(\text{TiO}_2)_{38}$ system. Two O atoms in the B-ring bond to the five-coordinated Ti (Ti5c). The proton dissociated from the B-ring is adsorbed onto the two-coordinated O (O2c) in the semiconductor.

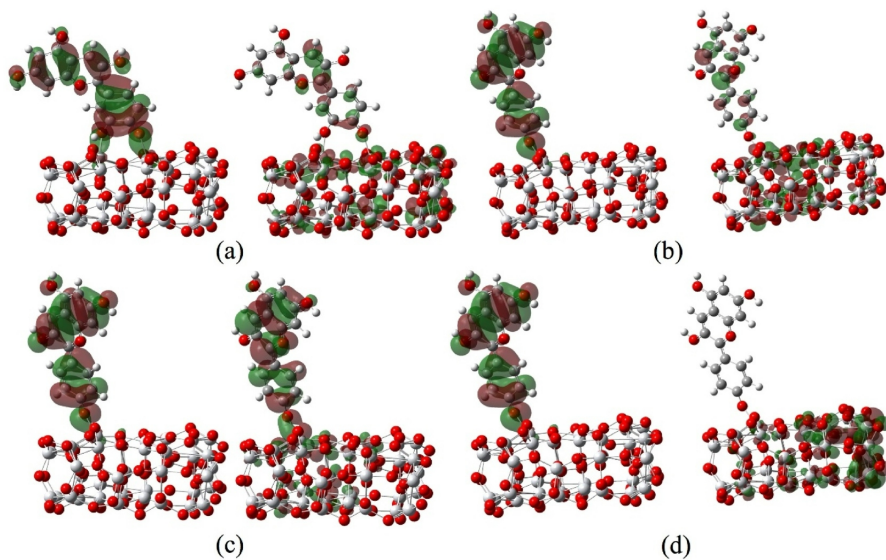


Fig. 4. Natural transition orbitals for (a) the sixth excited state of cyanidin/ $(\text{TiO}_2)_{38}$, and (b) the first, (c) second, and (d) third excited states of pelargonidin/ $(\text{TiO}_2)_{38}$. The hole (left) and particle (right) are shown, where the eigenvalues of these pairs are larger than 0.98 and thus the transitions are characterized by one single pair.

Supplementary Material

Characterization of dye-sensitized solar cells using five pure anthocyanidin 3-*O*-glucosides possessing different chromophores

Yuki Kimura^a, Takeshi Maeda^a, Satoru Iuchi^a, Nobuaki Koga^a, Yasujiro Murata^b, Atsushi Wakamiya^b, Kumi Yoshida^{a*}

^aGraduate School of Information Science, Nagoya University, Chikusa, Nagoya 464-8601, Japan

^bInstitute for Chemical Research, Kyoto University, Uji, Kyoto 611-0011, Japan

*Correspondence author: FAX +81-52-789-5638; E-mail yoshidak@is.nagoya-u.ac.jp

Table S1.

Photovoltaic properties of the DSSCs sensitized with anthocyanins (**1-5**) using a cobalt electrolyte ($\text{Co}^{2+}/\text{Co}^{3+}$).

Dye ^a	J_{sc} (mA/cm ²)	V_{oc} (mV)	FF	η (%)
Pg3G	0.21	208	0.42	0.02
Cy3G	0.30	255	0.44	0.03
Dp3G	0.46	263	0.43	0.05
Pt3G	0.33	246	0.44	0.04
Mv3G	0.18	227	0.44	0.02

^aDyes were dissolved in each solvent with the concentration of 0.5 mM and immersed at rt for 18 h.

Table S2.

Absorption energies (eV), oscillator strengths f , and transition characters of the singlet excited states of the delphinidin, petunidin, malvidin and dye/(TiO₂)₃₈ systems.

state	energy ^a	f	assignment ^b
delphinidin			
1	2.51 (494)	0.6663	H→L (92%)
delphinidin/(TiO ₂) ₃₈			
1	2.07 (598)	0.1900	H→L (52%)
2	2.10 (591)	0.0737	H→L+2 (80%)
3	2.15 (577)	0.3839	H→L+1 (71%)
4	2.19 (566)	0.0070	H→L+3 (54%)
5	2.25 (552)	0.0468	H→L+4 (20%), H→L+5 (26%)
6	2.30 (539)	0.1930	H→L+4 (47%)
petunidin			
1	2.45 (505)	0.6605	H→L (93%)
petunidin/(TiO ₂) ₃₈			
1	2.03 (611)	0.1722	H→L (60%)
2	2.07 (599)	0.0204	H→L+2 (92%)
3	2.11 (587)	0.3876	H→L+1 (76%)
4	2.15 (576)	0.0225	H→L+3 (58%)
5	2.20 (564)	0.0491	H→L+5 (28%), H→L+6 (23%)
6	2.27 (547)	0.1801	H→L+4 (54%)
malvidin			
1	2.46 (504)	0.7380	H→L (94%)
malvidin/(TiO ₂) ₃₈			
1	2.10 (591)	0.0380	H→L (58%), H→L+2 (30%)
2	2.21 (561)	0.5990	H→L (34%), H→L+2 (37%)
3	2.23 (557)	0.1972	H→L+1 (73%), H→L+2 (22%)
4	2.30 (538)	0.0230	H→L+3 (53%), H→L+8 (21%)
5	2.31(536)	0.1822	H→L+3 (32%), H→L+8 (27%)

^aValues in nm are given in parentheses.

^bContributions above 20% are presented. H and L represent HOMO and LUMO, respectively.

Table S3.

Orbital energies ϵ (eV) and contributions (%) of the dye atomic orbitals for delphinidin/(TiO₂)₃₈, petunidin/(TiO₂)₃₈ and malvidin/(TiO₂)₃₈ with C-PCM.

orbital	ϵ (eV)	weight (%)
delphinidin/(TiO ₂) ₃₈		
LUMO+6	-2.86	1
LUMO+5	-2.90	2
LUMO+4	-2.92	5
LUMO+3	-2.96	2
LUMO+2	-3.06	0
LUMO+1	-3.11	19
LUMO	-3.14	60
HOMO	-5.54	95
petunidin/(TiO ₂) ₃₈		
LUMO+6	-2.85	1
LUMO+5	-2.89	3
LUMO+4	-2.91	7
LUMO+3	-2.95	1
LUMO+2	-3.04	0
LUMO+1	-3.10	26
LUMO	-3.12	49
HOMO	-5.49	95
malvidin/(TiO ₂) ₃₈		
LUMO+8	-2.80	0
LUMO+7	-2.84	1
LUMO+6	-2.85	0
LUMO+5	-2.89	0
LUMO+4	-2.90	0
LUMO+3	-2.98	2
LUMO+2	-3.07	10
LUMO+1	-3.10	38
LUMO	-3.13	41
HOMO	-5.55	97

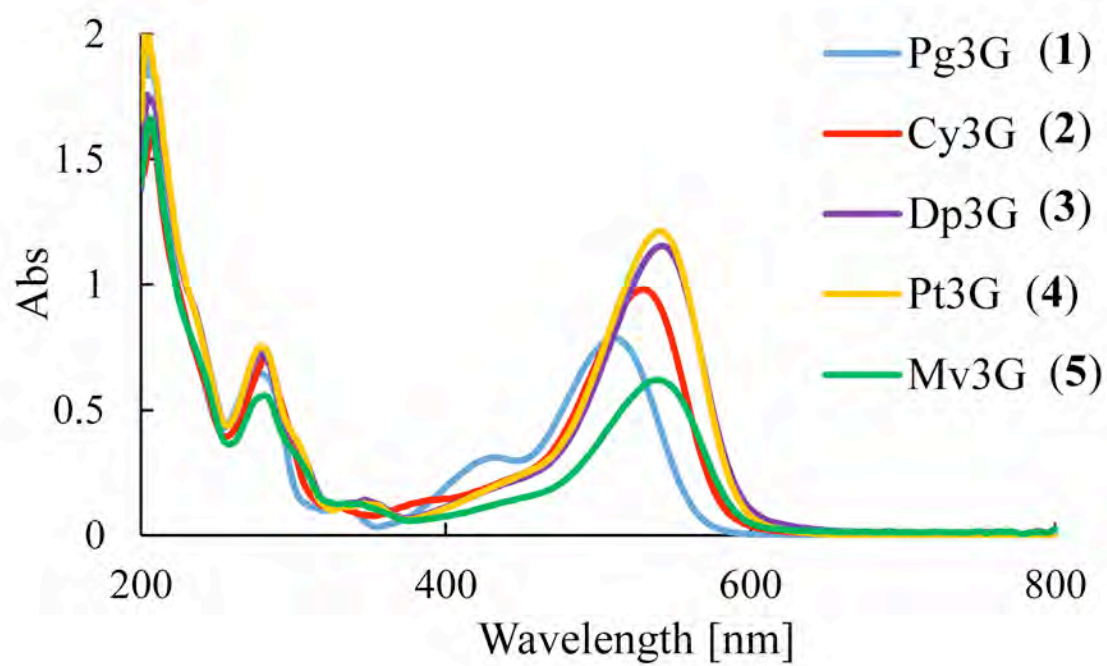


Fig. S1. The UV-vis spectra of the TFA salts of anthocyanins (1-5) in MeOH at the concentration of 0.5 mM (cell length: 10 mm).

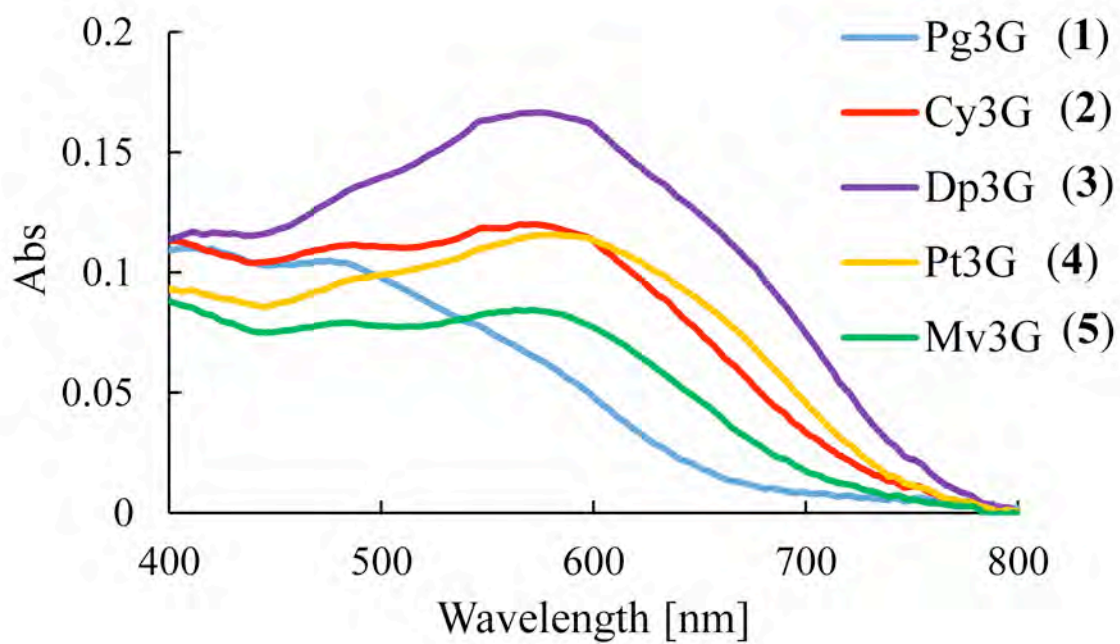


Fig. S2. The reflection spectra of anthocyanins-adsorbed TiO₂ electrodes.

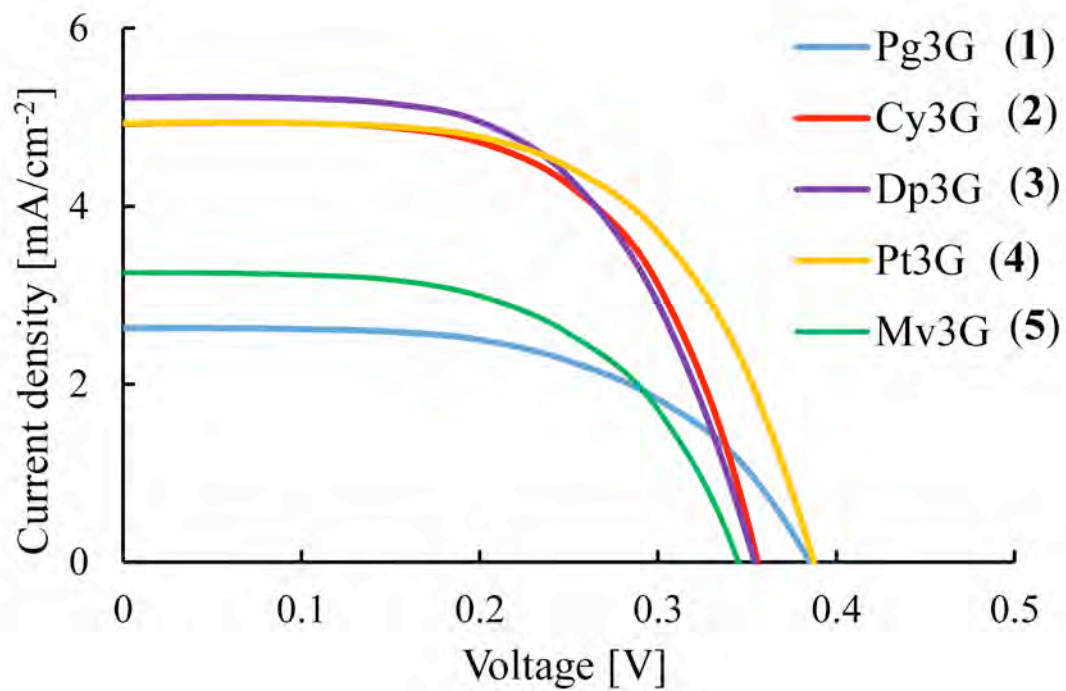


Fig. S3. Current-voltage curves of the DSSCs sensitized with anthocyanins (1-5) without TBP. To immerse dyes (2-5) MeOH was used, and PrOH was used in the case of Pg3G (1).

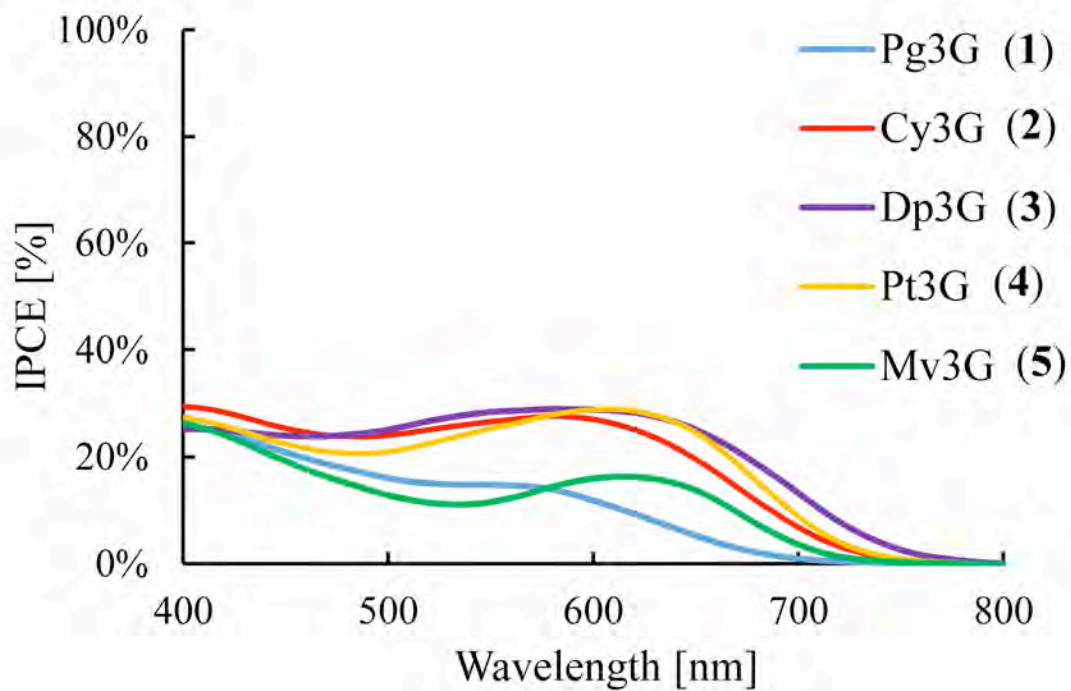


Fig. S4. IPCE spectra of the DSSCs sensitized with anthocyanins (1-5) without TBP. To immerse dyes (2-5) MeOH was used, and PrOH was used in the case of Pg3G (1).

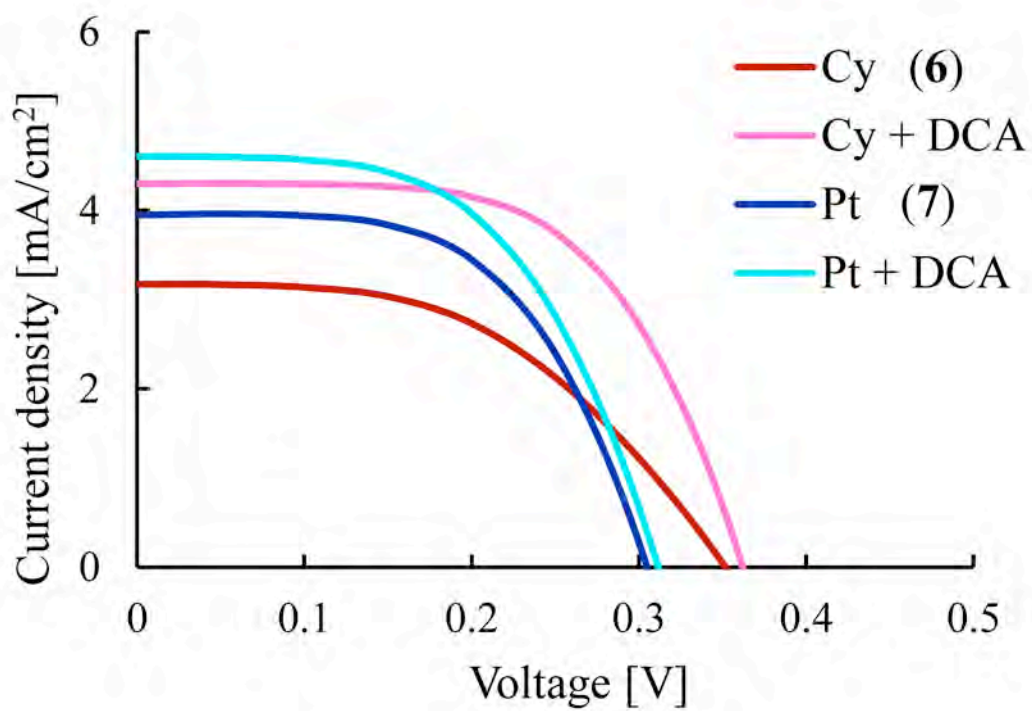


Fig. S5. Current-voltage curves of the DSSCs sensitized with anthocyanidins (**6**, **7**), with and without DCA.

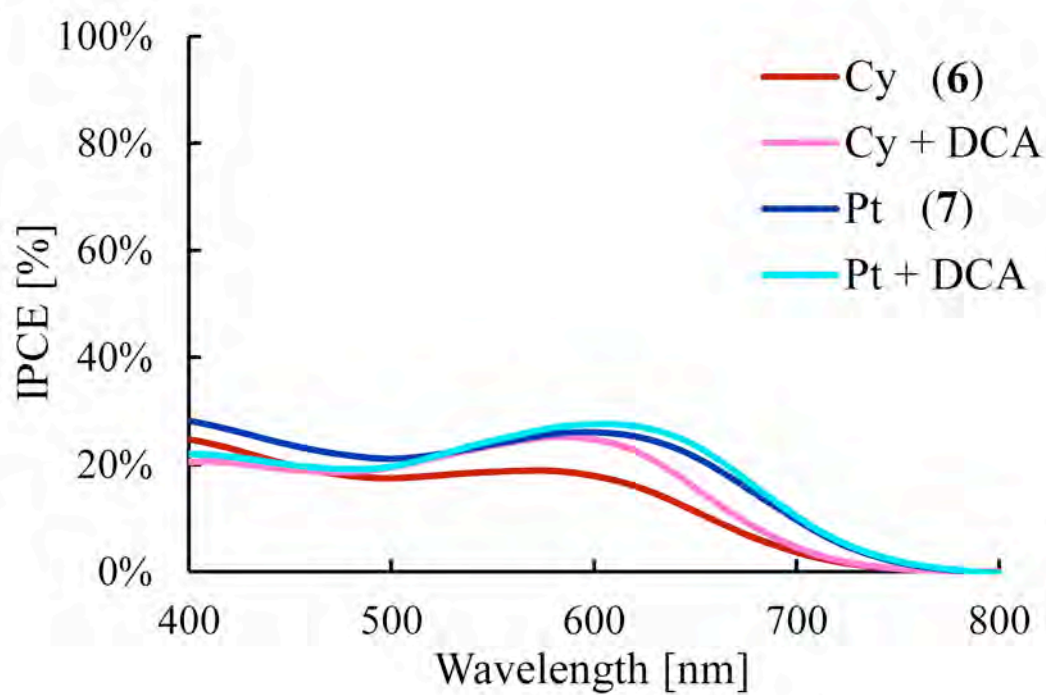


Fig. S6. IPCE spectra of the DSSCs sensitized with anthocyanidins (6, 7), with and without DCA.

Highlights

- DSSCs using five pure anthocyanidin 3-*O*-glucosides were prepared and characterized.
- All the anthocyanins gave beautiful purple to blue color cells.
- Petunidin 3-*O*-glucoside exhibit the highest η (%) of 1.42% with DCA without TBP.
- TD-DFT calculations of anthocyanidin dyes on a (TiO₂)₃₈ cluster were performed.
- Both indirect and direct electron injection mechanisms might co-exist.